Rpl33, a Nonessential Plastid-Encoded Ribosomal Protein in Tobacco, Is Required under Cold Stress Conditions [W][OA]

Marcelo Rogalski, Mark A. Schöttler, Wolfram Thiele, Waltraud X. Schulze, and Ralph Bock[1]

Max-Planck-Institut für Molekulare Pflanzenphysiologie, D-14476 Potsdam-Golm, Germany

Plastid genomes contain a conserved set of genes encoding components of the translational apparatus. While knockout of plastid translation is lethal in tobacco (*Nicotiana tabacum*), it is not known whether each individual component of the plastid ribosome is essential. Here, we used reverse genetics to test whether several plastid genome–encoded ribosomal proteins are essential. We found that, while ribosomal proteins Rps2, Rps4, and Rpl20 are essential for cell survival, knockout of the gene encoding ribosomal protein Rpl33 did not affect plant viability and growth under standard conditions. However, when plants were exposed to low temperature stress, recovery of Rpl33 knockout plants was severely compromised, indicating that Rpl33 is required for sustaining sufficient plastid translation capacity in the cold. These findings uncover an important role for plastid translation in plant tolerance to chilling stress.

INTRODUCTION

Plastids (best known in their green differentiation form, the chloroplasts) have retained a small prokaryotic-type genome from their cyanobacterial ancestors. The plastid genome (plastome) is identical in all plastid types and occurs at high copy numbers with up to thousands of genome copies being present in a single cell. The plastomes of vascular plants display little size variation and contain a conserved set of ~120 genes (Bock, 2007). Protein biosynthesis in plastids is performed in the stroma on prokaryotic-type 70S ribosomes (Peled-Zehavi and Danon, 2007). While all RNA components of these ribosomes (the 16S rRNA of the small ribosomal subunit and the 23S, 5S, and 4.5S rRNAs of the large subunit) are encoded by the plastid genome, only a subset of the ribosomal proteins is plastome encoded. In tobacco (*Nicotiana tabacum*) and most other higher plants, 12 of the 25 proteins in the small ribosomal subunit (30S) and nine of the 33 proteins in the large ribosomal subunit (50S) are encoded by plastid genes. In addition to these classical ribosomal proteins, plastids also possess a small set of ribosome-associated proteins that are not found in bacterial 70S ribosomes and therefore are referred to as plastid-specific ribosomal proteins (Yamaguchi et al., 2000; Yamaguchi and Subramanian, 2000; Manuell et al., 2007; Sharma et al., 2007).

Recent work has demonstrated that plastid translation is essential for cell survival in tobacco plants. Knockout of plastid translation by plastome transformation resulted in characteristic phenotypic aberrations (Ahlert et al., 2003; Rogalski et al., 2006).

Somatic segregation of plastid genomes toward homoplasmy of the knockout (i.e., segregation into cells that lack any residual wild-type plastome copies) led to cell death, which in turn caused severe organ deformations. Similar phenotypes were observed when targeted inactivation of essential plastid-encoded tRNA genes was attempted (Legen et al., 2007; Rogalski et al., 2008), supporting the notion that plastid translation is indispensable for cellular viability in tobacco plants.
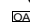
Although abolishing plastid protein biosynthesis is lethal, each individual component of the plastid ribosome may not be essential. Here, we adopted a reverse genetics approach to test which of several plastid-encoded ribosomal proteins are essential for survival. We specifically identified and included proteins that are candidates for not being essential constituents of the plastid ribosome. Such candidates were identified by two criteria. First, the protein should not be highly connected within the RNA and protein interaction landscape of the ribosome. Second, loss of the encoding gene from the plastomes of nonphotosynthetic plastid-containing organisms (such as holoparasitic plants and apicoplast-containing protozoa; Wilson, 2002; Bungard, 2004) could indicate that the protein is nonessential, at least under heterotrophic growth conditions. As most plastid genes are either directly or indirectly involved in supporting photosynthesis (Bock, 2007), it seems conceivable that there would be a much lower demand for plastid protein biosynthesis in nonphotosynthetic organisms. Thus, somewhat less efficient ribosomes could provide sufficient basal translational capacity to support the few nonphotosynthetic functions of the plastid genome (e.g., fatty acid biosynthesis, for which a plastome-encoded acetyl-CoA carboxylase subunit is required; Kode et al., 2005).

Using these criteria, we selected two ribosomal proteins of the large subunit (L20 and L33) and one of the small subunit (S2) for targeted inactivation of their corresponding genes in tobacco plastids. *rpl20* (for *ribosomal protein of the large subunit number 20*), the gene encoding the ribosomal protein L20 (Rpl20) is

absent from the plastid genomes of the parasitic protozoans *Eimeria tenella* (full genome accession number NC_004823), *Theileria parva* (full genome accession number NC_007758), and *Toxoplasma gondii* (full genome accession number NC_001799; Wilson et al., 1996; Wilson and Williamson, 1997; Wilson, 2002). Likewise, *rpl33*, the gene for protein L33 (Rpl33) is absent from the *T. gondii* plastid genome and from that of the colorless heterotrophic alga *Euglena longa* (also known as *Astasia longa*; Gockel et al., 1994; full genome accession number NC_002652). Interestingly, a functional *rpl33* gene is also absent from the plastomes of several phototrophic organisms, such as the green alga *Euglena gracilis* (full genome accession number NC_001603; Hallick et al., 1993) and the common bean (*Phaseolus vulgaris*), where it has degraded into a pseudogene (full genome accession number NC_009259; Guo et al., 2007). From the ribosomal proteins of the small subunit, we selected S2 (Rps2) encoded by the plastid *rps2* gene (for *ribosomal protein of the small subunit number 2*), which is the last protein to assemble into the 30S subunit of the *Escherichia coli* ribosome (Kaczanowska and Rydén-Aulin, 2007). Furthermore, the *rps2* gene is absent from the plastome of the parasitic, nonphotosynthetic green alga, *Helicosporidium* (full genome accession number NC_008100; de Koning and Keeling, 2006). As a control for a presumably essential ribosomal protein, we selected S4 (Rps4), which directly binds to 16S rRNA and is required early in the 30S assembly process (Kaczanowska and Rydén-Aulin, 2007).

Here, we report that, while S2, S4, and L20 represent essential components of the plastid ribosome, L33 is not required for plastid translation under normal growth conditions. However, *rpl33* knockout plants are severely compromised when exposed to chilling stress, suggesting that L33 is beneficial under certain environmental conditions and that plastid translation may be involved in tolerance to chilling stress.

RESULTS

Targeted Disruption of Four Plastid Ribosomal Protein Genes

We produced knockout alleles of *rpl20*, *rpl33*, *rps2*, and *rps4* and introduced them into the tobacco plastid genome by biolistic chloroplast transformation, where they replaced the corresponding wild-type alleles by homologous recombination (Bock and Khan, 2004; Maliga, 2004). The knockout alleles were constructed by subcloning the corresponding regions of the tobacco plastid DNA and replacing or disrupting the genes for the four ribosomal proteins with a chimeric selectable marker gene, *aadA* (Figures 1 to 4). The *aadA* gene product confers resistance to the aminoglycoside antibiotics spectinomycin and streptomycin and, when fused to chloroplast-specific expression signals, serves as a selectable marker for plastid transformation (Svab and Maliga, 1993). For each knockout construct, five to six independently generated transplastomic lines were selected for further analyses and designated as Δ*rps2*, Δ*rps4*, Δ*rpl20*, and Δ*rpl33* lines, respectively.

The primary transplastomic lines were subjected to additional rounds of regeneration and selection to enrich for the transgenic plastid genome and select against residual wild-type plastomes. Typically, this procedure results in homoplasmic transplastomic lines after two to three rounds of selection and regeneration (Svab and Maliga, 1993; Bock, 2001; Maliga, 2004).

Δ*rps2*, Δ*rps4*, and Δ*rpl20* Plants Remain Heteroplasmic

To investigate whether several rounds of stringent antibiotic selection had successfully eliminated all wild-type plastid genomes, we tested DNA samples from five to six transplastomic lines per construct by restriction fragment length polymorphism (RFLP) analyses.

When five Δ*rps4* transplastomic lines were analyzed, all of them showed novel fragments that were larger than the corresponding restriction fragments in the wild type, suggesting that they carry the *aadA* marker gene inserted into the *rps4* locus (Figure 1D). In addition, all lines had a hybridization signal for the wild-type restriction fragment even after three to four regeneration rounds, indicating that a plant cannot regenerate and survive if the *rps4* gene is eliminated from all plastid genomes.

The relative intensities of the hybridization signals for the wild-type plastome and the transplastome were very similar in all five transplastomic lines (and in different regeneration rounds; Figure 1D), indicating a balancing selection in which both genome types must be maintained: the transplastome to provide the spectinomycin resistance and the wild-type plastome to provide the presumably essential S4 protein. A similar stable heteroplasmy caused by balancing selection was observed previously when essential plastid genes were targeted in knockout experiments (Drescher et al., 2000; Rogalski et al., 2006, 2008).

Interestingly, in our RFLP analyses, two of the five transplastomic lines displayed a 2.5-kb band instead of the expected 2.8-kb fragment (Figures 1B and 1D). This band is the result of recombination between the (*psbA*-derived) 3′ untranslated region (UTR) of the *aadA* gene and that of the endogenous *psbA* gene, a phenomenon that has been reported previously (Rogalski et al., 2006). PCR analysis confirmed that recombination was the cause of the 2.5-kb hybridization signal (Figure 1C; see Supplemental Figure 1 online).

Attempts to knockout essential plastid genes result in characteristic phenotypes (Shikanai et al., 2001; Kode et al., 2005; Rogalski et al., 2006, 2008). When grown in soil, these plants frequently display aberrant leaf morphologies with large sectors of the leaf blade missing. This is because random segregation of plastid genomes regularly produces homoplasmic knockout cells, and, since these cells do not survive, the resulting lack of entire cell lineages during leaf development produces severely misshapen leaves (Shikanai et al., 2001; Kode et al., 2005; Rogalski et al., 2006, 2008). When Δ*rps4* transplastomic lines were grown in the greenhouse, we frequently noticed these typical phenotypic aberrations (Figure 1D), ultimately confirming that *rps4* is essential for plastid translation and ribosome function.

We had expected *rps4* to be essential, because the S4 protein is required early in the assembly process of the 30S ribosomal subunit and directly binds to the 16S rRNA (Kaczanowska and Rydén-Aulin, 2007). We next analyzed the Δ*rps2* and Δ*rpl20* transplastomic lines (Figures 2 and 3). Both of these genes were
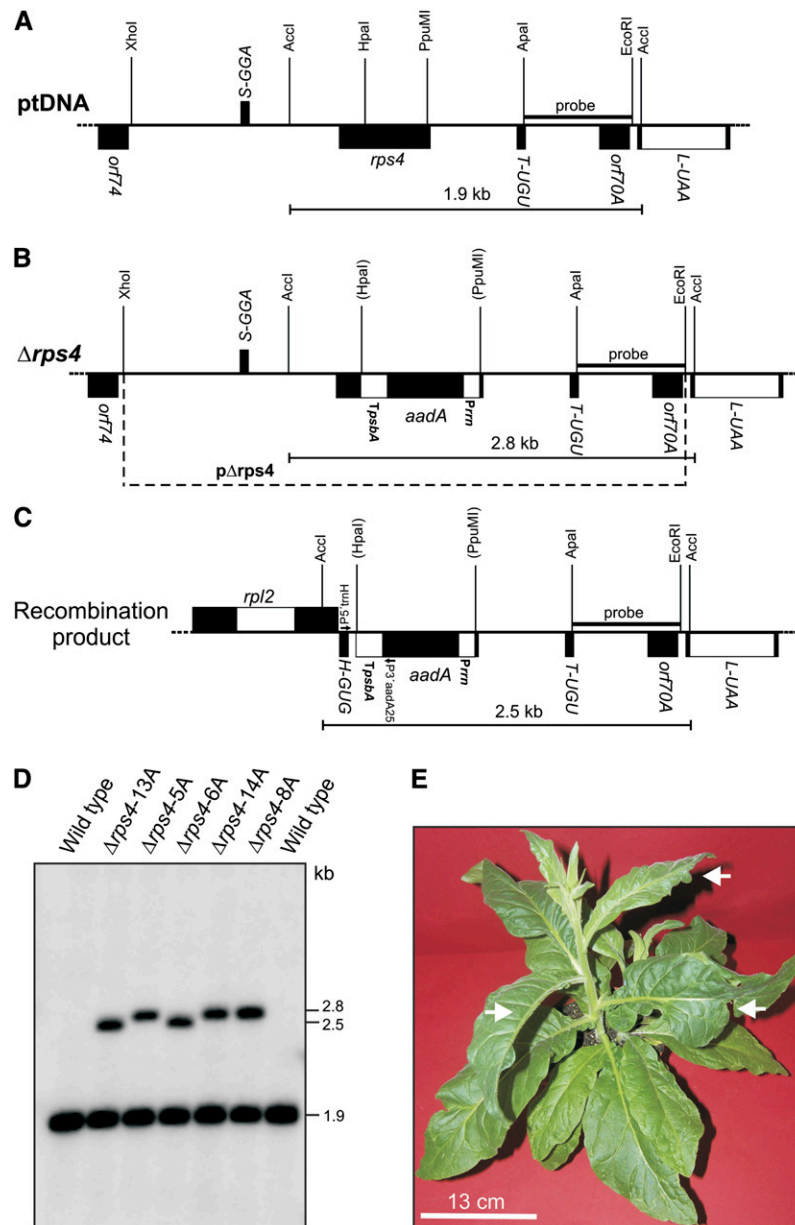
Figure 1. Targeted Inactivation of the *rps4* Gene Encoding Plastid Ribosomal Protein S4.
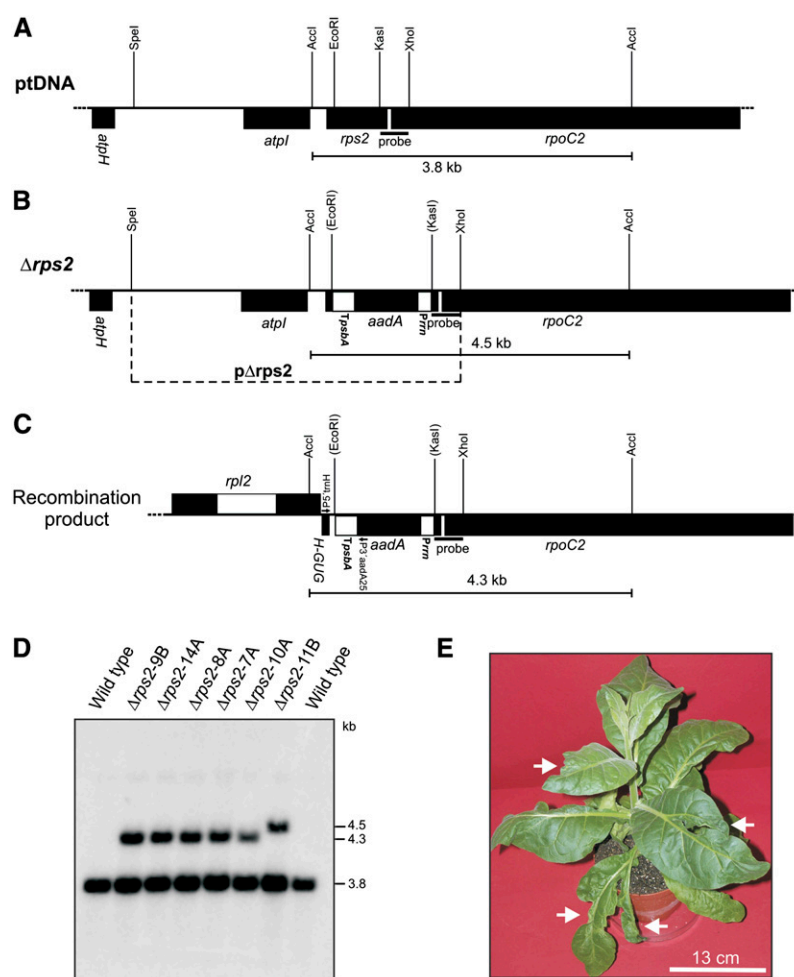
(A) Physical map of the region in the tobacco plastid genome (ptDNA; Shinozaki et al., 1986) containing the *rps4* gene. Genes above the lines are transcribed from the left to the right; genes below the lines are transcribed in the opposite direction. Filled boxes represent genes and open reading frames (*orf*).

(B) Map of the transformed plastid genome region produced with plastid transformation vector p*Δrps4*. The chloroplast targeting fragment in the transformation vector is marked by dashed lines (*XhoI/Eco*RI fragment). The selectable marker gene *aadA* is driven by the rRNA operon-derived chimeric P*rrn* promoter (Svab and Maliga, 1993) and fused to the 3′UTR from the plastid *psbA* gene (T*psbA*; open boxes). Restriction sites used for cloning, RFLP analysis, and/or generation of hybridization probes are indicated. Sites lost due to ligation to heterologous ends are shown in parentheses.

(C) Map of the recombination product arising from homologous recombination between the *psbA* 3′UTR of the chimeric *aadA* gene and the 3′UTR of the endogenous *psbA* gene. PCR primers used to confirm recombination are indicated (arrows; PCR products are presented in Supplemental Figure 1 online). The hybridization probe (*ApaI/Eco*RI fragment) is marked by a horizontal bar, and the expected sizes of hybridizing bands in the RFLP analysis are shown below each map.

(D) RFLP analysis of plastid transformants. All lines are heteroplasmic and show the 1.9-kb wild-type–specific hybridization band. Recombination has occurred in lines 13A and 6A. DNA samples from individual transplastomic lines were isolated after three or four regeneration rounds. A and B designate individual plants regenerated from a given transplastomic line.

(E) Phenotype of a typical *Δrps4* transplastomic plant ∼4 weeks after transfer from sterile culture to the greenhouse. Arrows point to misshapen leaves.

Figure 2. Targeted Inactivation of the *rps2* Gene Encoding Plastid Ribosomal Protein S2.

(A) Physical map of the region in the tobacco plastome (ptDNA) containing *rps2*. Transcriptional orientations and labeling of restriction sites, vector sequences, primers, hybridization probes, and hybridizing fragments are as in Figure 1.
(B) Map of the relevant region of the transformed plastid genome produced with plastid transformation vector pΔ*rps2*.
(C) Map of the recombination product.
(D) RFLP analysis of plastid transformants. All lines are heteroplasmic, as indicated by the presence of the 3.8-kb wild-type–specific hybridization signal. Recombination has occurred in lines 9B, 14A, 8A, 7A, and 10A (see Supplemental Figure 1 online).
(E) Phenotype of a representative Δ*rps2* transplastomic plant. Arrows point to deformed leaves.

also shown to be essential, as evidenced by stable heteroplasmy in DNA gel blot hybridizations (Figures 2D and 3D) and the leaf deformations typically seen in knockout transformants for essential plastid genes (Figures 2E and 3E). This indicates that, in spite of the loss of the *rpl20* and *rps2* genes from the plastomes of some plastid-containing unicellular eukaryotes and despite the late incorporation of S2 into the S30 subunit, both Rpl20 and Rps2 are indispensable for ribosome function in higher plant plastids.

Rpl33 Is a Nonessential Plastid Ribosomal Protein

We next analyzed the Δ*rpl33* transplastomic lines. DNA gel blot analysis of DNA from six independently generated Δ*rpl33* lines

that had undergone three rounds of regeneration did not produce a hybridization signal for the wild-type genome (Figure 4C). This tentatively suggested that all wild-type plastomes had successfully been eliminated from these lines. Homoplasmy of the *rpl33* knockout plastome indicates that, in contrast with the other three genes evaluated, *rpl33* is not essential for cell survival and, hence, probably not required for maintenance of plastid translation.

To confirm that we had succeeded in producing an *rpl33* knockout by targeted inactivation, we amplified both borders of the insertion site of the *aadA* marker (Figures 4A, 4B, and 4D). The PCR data verified the successful deletion of *rpl33* from the plastid genome and its replacement with the selection marker *aadA* by homologous recombination (Figure 4D).
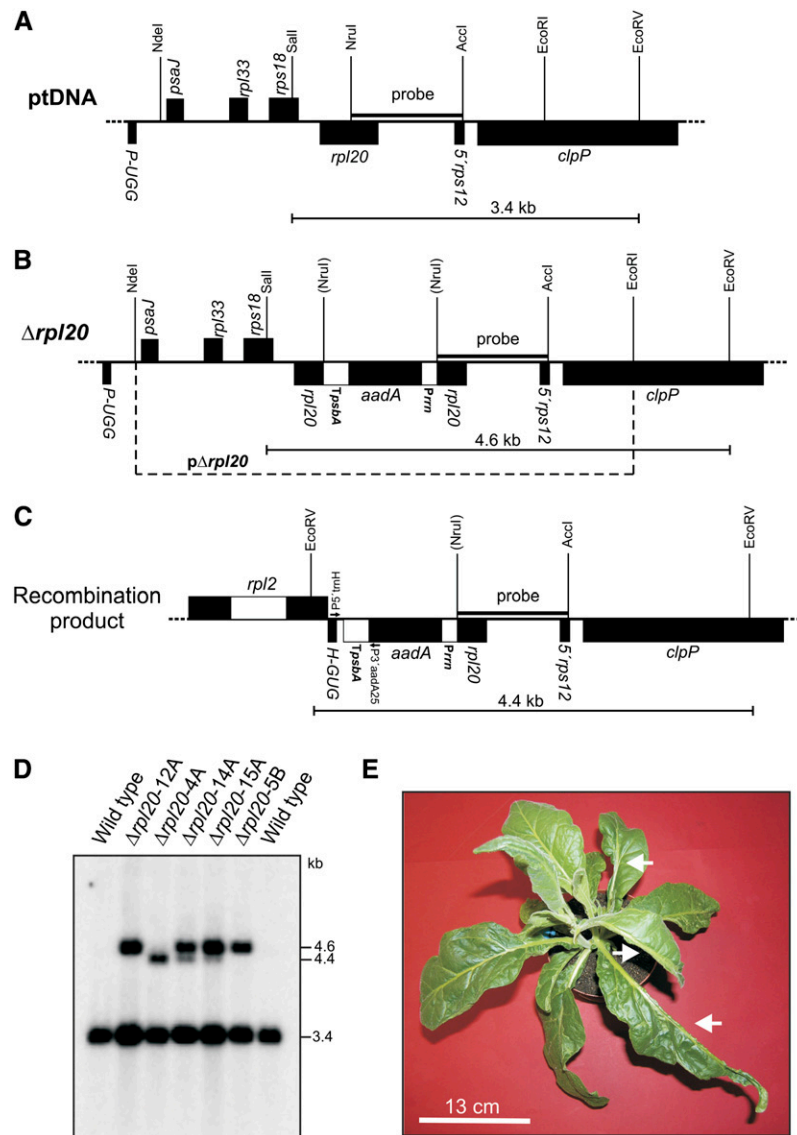
Figure 3. Targeted Inactivation of the *rpl20* Gene Encoding Plastid Ribosomal Protein L20.

(A) Physical map of the region in the tobacco plastid DNA (ptDNA) containing *rpl20*. Transcriptional orientations and labeling of restriction sites, vector sequences, primers, hybridization probes, and hybridizing fragments are as in Figure 1.
(B) Map of the transformed region of the plastid genome produced with plastid transformation vector pΔ*rpl20*.
**(C)** Map of the recombination product.
(D) RFLP analysis of plastid transformants. All lines are heteroplasmic, as evident from the presence of the 3.4-kb hybridization signal diagnostic of the wild-type plastome. Recombination has occurred in line 4A and, to a limited extent, also in lines 14A and 15A (see Supplemental Figure 1 online).
(E) Phenotype of a representative Δ*rpl20* transplastomic plant. Arrows point to phenotypically abnormal leaves lacking sectors of the leaf blade.

Finally, we wanted to obtain genetic confirmation that the *rpl33* knockout was homoplasmic. We thus performed inheritance tests, which are the most sensitive means of assessing homoplasmy versus heteroplasmy (Svab and Maliga, 1993; Bock, 2001). As controls, we included wild-type seed samples and seeds from the heteroplasmic Δ*rps2*, Δ*rps4*, and Δ*rpl20* lines (Figure 5). As expected, transmission of the *rps2*, *rps4*, and *rpl20* knockout alleles into the T1 generation (obtained by selfing of

regenerated transplastomic plants) turned out to be very low (Figures 5C to 5E), indicating that the knockout allele is strongly selected against, and, in the absence of spectinomycin selection, the knockout plastome is quickly lost and displaced by wild-type genome copies. The cotyledons of the few surviving seedlings were usually variegated, suggesting that the seedlings are heteroplasmic and contain sectors with wild-type chloroplasts only, which bleach out in the presence of the antibiotic
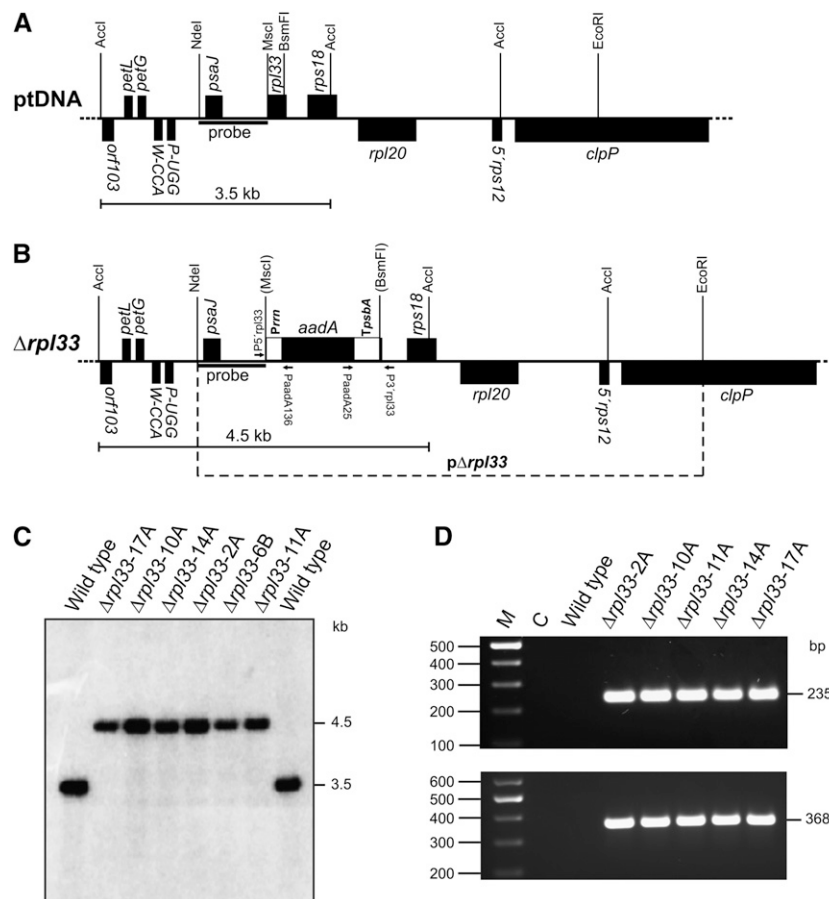
Figure 4. Targeted Inactivation of the *rpl33* Gene Encoding Plastid Ribosomal Protein L33.

(A) Physical map of the region in the tobacco plastome (ptDNA) containing *rpl33*. Transcriptional orientations and labeling of restriction sites, vector sequences, primers, hybridization probes, and hybridizing fragments are as in Figure 1.

(B) Map of the transformed plastid genome produced with plastid transformation vector pΔ*rpl33*.

(C) RFLP analysis of plastid transformants. Absence of the wild-type–specific 3.5-kb hybridization signal from all Δ*rpl33* lines indicates homoplasmy of the *rpl33* deletion.

(D) Confirmation of the *rpl33* knockout by PCR. Amplification with primer pair P5′rpl33 and PaadA136 produces the expected 235-bp PCR product in all transplastomic lines (top panel). Likewise, PCR with primer pair PaadA25 and P3′rpl33 yields the expected 368-bp amplification product (bottom panel). C, buffer control.

(Figures 5C to 5E). By contrast, germination of seeds from Δ*rpl33* lines on spectinomycin-containing medium yielded a uniform population of homogeneously green seedlings (Figure 5F). This lack of phenotypic segregation in the T1 generation provides strong additional evidence of homoplasmy and genetic stability of the *rpl33* knockout lines.

L33 Is Not Required for Efficient Translation under Standard Conditions

Having successfully generated homoplasmic *rpl33* deletion lines, we were interested in assessing the phenotypic consequences of losing the L33 protein from plastid ribosomes. Surprisingly, when Δ*rpl33* transplastomic lines were grown under standard greenhouse conditions, they showed no visible phenotype during any stage of development (Figure 6). Plant growth

rates, development, and onset of flowering were identical to wild-type plants (Figure 6C), indicating that L33 is dispensable under standard growth conditions.

To confirm that plastid translation proceeds faithfully in the absence of the L33 protein, we conducted polysome loading analyses (Figure 7). These assays measure the coverage of mRNAs with ribosomes and, in this way, represent a measure of translational activity (Barkan, 1988, 1998). When we compared ribosome association of four plastid transcripts (*psbA*, encoding the D1 protein of photosystem II; *rbcL*, encoding the large subunit of ribulose-1,5-bis-phosphate carboxylase/oxygenase; the dicistronic *psaA/B* mRNA, encoding the two reaction center proteins of photosystem I; and the *psbE* operon transcript, a tetracistronic mRNA encoding four small subunits of photosystem II) in polysome preparations from wild-type and mutant plants, no strong difference in ribosome loading was detected
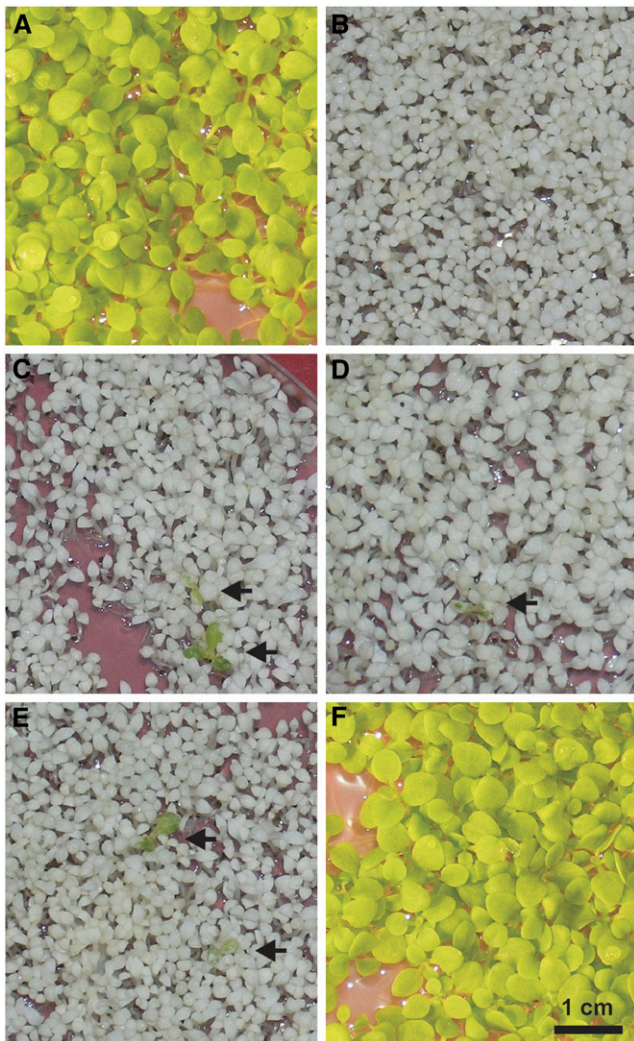
Figure 5. Seed Assays Assessing Homoplasmy versus Heteroplasmy of Transplastomic Lines.

(A) Wild-type control on medium without spectinomycin.

(B) Wild-type control on medium with spectinomycin.

(C) Seeds from a Δ*rps4* transplastomic line on spectinomycin-containing medium. Spectinomycin-resistant seedlings (black arrows) are green or green-white variegated.

(D) Seeds from a Δ*rps2* transplastomic line on spectinomycin-containing medium.

(E) Seeds from a Δ*rpl20* transplastomic line on spectinomycin-containing medium. The rare appearance of spectinomycin-resistant seedlings in Δ*rps4*, Δ*rps2*, and Δ*rpl20* lines indicates that, in the absence of antibiotic selection, the transgenic plastid genome is rapidly lost after transfer from antibiotic-containing synthetic medium to soil.

(F) Seeds from a Δ*rpl33* transplastomic line on spectinomycin-containing medium. All seedlings are green, which confirms that the *rpl33* knockout is homoplasmic.

(Figure 7) in that the polysome profiles (i.e., the mRNA distribution across the sucrose density gradient) were very similar. This provides further evidence that L33 lacks an important function in the ribosome under standard growth conditions and is consistent with the normal appearance of the Δ*rpl33* knockout lines (Figure 6). However, we reproducibly detected subtle differences between polysomal profiles in the wild type and in the mutant. For example, fraction 3 of the wild type contained the most *psbE* mRNA, as opposed to fraction 2 of the mutant. Similarly, the *psaA/B* mRNA peaks in fraction 5 of the wild type but in fraction 4 of the mutant. Furthermore, the *rbcL* mRNA distribution is slightly shifted toward the upper gradient fractions in the mutant (Figure 7). This may suggest that ribosome loading of mRNAs in the Δ*rpl33* mutant is slightly less intense than in the wild type.

We have considered the possibility that a copy of the *rpl33* gene was transferred to the nucleus, became functional there, and, in this way, made the plastid *rpl33* gene dispensable (Timmis et al., 2004; Bock, 2006). To exclude this possibility, we purified ribosomes from both wild-type tobacco plants and the Δ*rpl33* knockout. The proteins of the purified ribosomes were then separated in denaturing polyacrylamide gels, and all proteins with a molecular mass of between 5 and 22 kD were subjected to ribosomal protein identification by mass
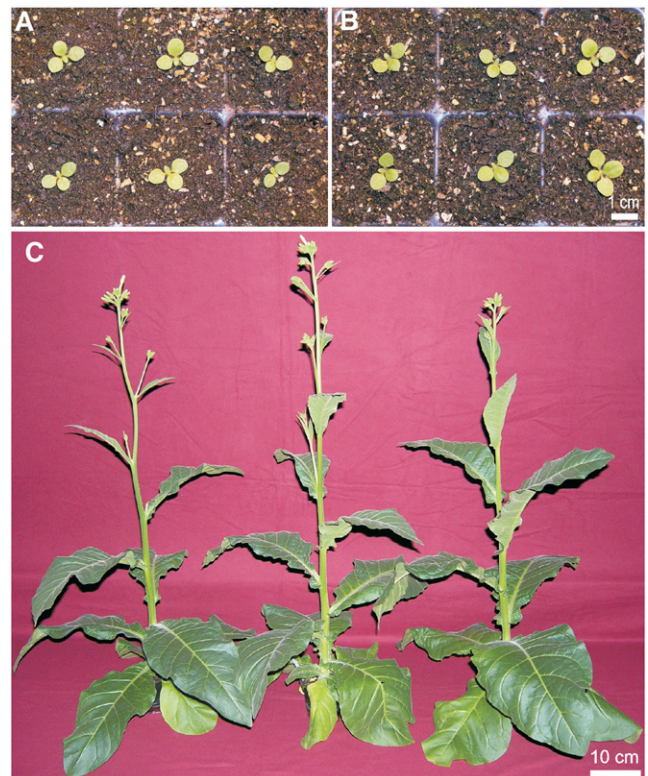
Figure 6. Phenotype of Δ*rpl33* Plants at Different Stages of Development.

(A) Wild-type seedlings.

(B) Δ*rpl33* seedlings.

(C) A wild-type plant (left) and two Δ*rpl33* knockout plants (center and right) at the onset of flowering.
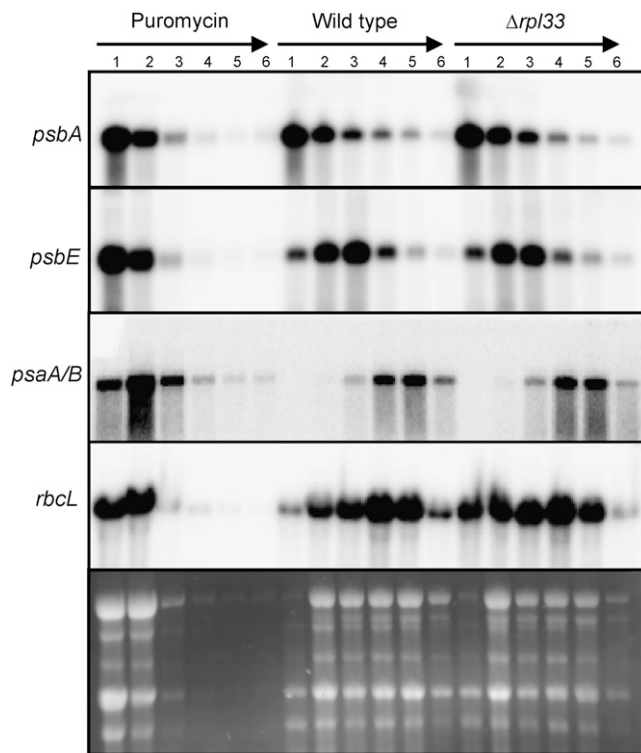
Figure 7. Polysome Loading Analysis to Assess Translational Activity in Δ*rpl33* Plants.

Polysome profiles are shown for four chloroplast transcripts: *psbA*, *psbE*, *psaA/B*, and *rbcL*. Polysome association of mRNAs was determined by fractionating the sucrose gradient in six fractions (numbered from top to bottom). Wild-type plants, Δ*rpl33* plants, and a wild-type control (labeled Puromycin), in which the polysomes were dissociated by treatment with the antibiotic puromycin, were analyzed. The horizontal arrows indicate the gradient fractionation from the top to the bottom. An ethidium bromide–stained agarose gel prior to blotting is shown at the bottom.

spectrometry. In this analysis, most ribosomal proteins with theoretical molecular masses between 5 and 22 kD were detected in both the wild type and the mutant, including 14 proteins of the small subunit (S6, S8, S10, S11, S12, S13, S14, S15, S16, S17, S18, S19, S20, and PSRP4) and 17 proteins of the large subunit (L9, L12, L14, L16, L17, L18, L22, L23, L27, L28, L29, L31, L32, L34, L35, L36, and PSRP6). While the L33 protein could be readily detected in ribosomes from the wild type (emPAI index: 5.35; Ishihama et al., 2005), no L33 was identifiable in ribosomes from the Δ*rpl33* knockout (see Supplemental Table 1 online), suggesting that the ribosomes in the mutant are indeed able to function without an L33 protein.

L33 Is Important for Recovery from Chilling Stress

As the plastid genome–encoded set of ribosomal proteins is highly conserved in higher plants (Bock, 2007), the finding that the L33 protein is altogether dispensable for chloroplast translation was unexpected. We suspected that, although L33 is apparently not needed under standard growth conditions, it may

become functionally relevant under specific conditions. Therefore, we tested a variety of different growth conditions, including a wide range of light and temperature conditions. Neither extreme low light nor high light (with tested light intensities ranging from 50 to 1100 μmol m^{-2} s^{-1}) had any discernable effect on either growth rate or development of the Δ*rpl33* knockout lines. As plastid ribosomes are known to be sensitive to heat stress (Feierabend, 1992; Falk et al., 1993), we compared the tolerance of wild-type and mutant plants to high-temperature stress of up to 37°C. However, no difference in phenotype or growth rates was observed, suggesting that L33 may not be involved in the stability of the plastid ribosome at elevated temperatures.

A recent study suggested that chilling stress interferes with protein biosynthesis in plastids by causing ribosome pausing and thereby delaying translation elongation (Grennan and Ort, 2007). To test whether L33 is involved in maintaining sufficient levels of chloroplast translation in the cold, we exposed wild-type plants and Δ*rpl33* knockout plants to continuous chilling stress of 4°C for 5 weeks. A period of 5 weeks had been determined as the optimum duration of the chilling stress treatment for tobacco, which we found to be significantly less sensitive to cold than, for example, *Arabidopsis thaliana*. Both wild-type and mutant plants showed a progressive loss of pigments in the cold but did not differ markedly from each other. However, after transferring the plants back to normal growth conditions, recovery of the Δ*rpl33* mutant plants from cold stress was severely compromised. While wild-type plants showed only mild stress symptoms and recovered quickly (Figures 8A and 8C), Δ*rpl33* knockout plants displayed strong symptoms of photooxidative damage and recovered much slower (Figures 8B and 8D). Although the mutant plants could eventually fully recover and continued to grow, their growth and development remained delayed compared with those of the wild type (Figure 8E).

Photosynthesis in Δ*rpl33* Knockout Plants

Most plastid-genome encoded genes are involved in either photosynthesis or gene expression (Wakasugi et al., 2001; Bock, 2007). To explore the basis for the observed chilling-sensitive phenotype, we measured photosynthetic performance in wild-type plants and the Δ*rpl33* knockout mutant. The accumulation of the protein complexes of the photosynthetic electron transport chain can be precisely quantified using sensitive spectroscopic methods (Schöttler et al., 2007a); thus, the efficiency of photosynthetic electron transport can serve as a more sensitive indicator of plastid translational efficiency than polysome loading analysis. No significant differences in photosynthetic complex accumulation were detected between mature leaves of wild-type and L33 mutant plants grown under standard conditions (Table 1). The Δ*rpl33* knockout mutant exhibited a slightly lower chlorophyll *a/b* ratio than the wild type, which, however, does not translate into a significant reduction in photosynthetic performance (Table 1, Figure 6).

Recent genetic analysis has established that efficient chloroplast translation is particularly important in young developing leaves (Albrecht et al., 2006; Rogalski et al., 2008). We therefore also measured photosynthesis in young expanding leaves of the wild type and the Δ*rpl33* knockout mutant. Interestingly, we
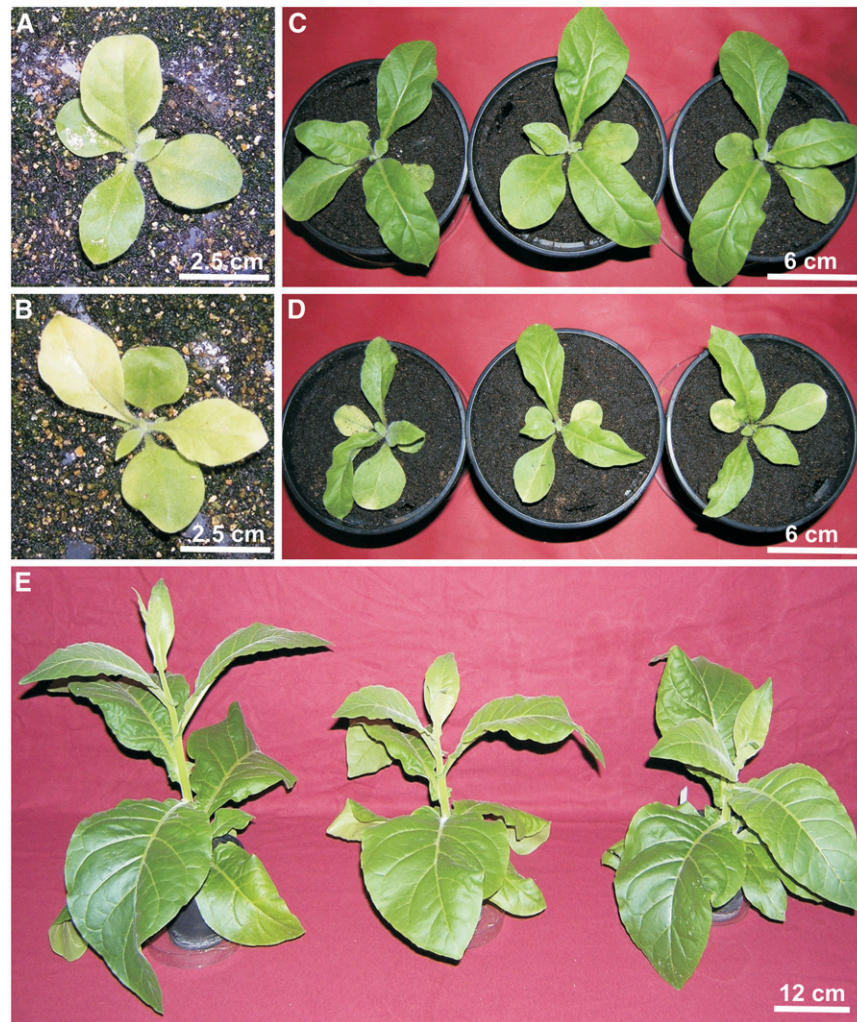
Figure 8. Development of Wild-Type and Δ*rpl33* Plants during Recovery from Cold Stress.

(A) and **(B)** A wild-type plant **(A)** and a Δ*rpl33* plant **(B)** grown for 5 d under normal growth conditions in the greenhouse after chilling stress.

(C) and **(D)** Wild-type **(C)** and Δ*rpl33* plants **(D)** after 10 d in the greenhouse. Note that the leaves at the base of the Δ*rpl33* plants are yellow.

(E) A wild-type plant (left) and two Δ*rpl33* knockout plants (center and right) after 25 d of growth in the greenhouse. Although the mutant plants have now fully recovered, their growth has been delayed.

observed differences between the photosynthetic parameters of young expanding leaves of the wild type and the mutant (Table 1). The chlorophyll content per leaf area and the quantum yield of dark adapted photosystem II (F_v/F_m, the ratio of variable to maximum fluorescence), a measure of photosystem II (PSII) integrity, are significantly reduced in the Δ*rpl33* knockout plants (Table 1). Also, the plastocyanin (PC) content relative to photosystem I (PSI) is elevated in the Δ*rpl33* knockout, as determined by difference absorption spectroscopy. The latter observation is most readily explained by a reduction in PSI content per leaf area in the Δ*rpl33* knockout, presumably due to less efficient synthesis of the chloroplast-encoded components of the photosynthetic apparatus. As PC is encoded in the nuclear genome, its accumulation is not affected by the absence of the L33 protein. Since the leaf chlorophyll content is 25% lower in young

expanding leaves of the Δ*rpl33* knockout than of the wild type (Table 1), it can be assumed that PSI is reduced to ~70% of wild-type levels on a leaf area basis (ΔI/I normalized to chlorophyll contents; Table 1). The increase in the PC:P_{700} ratio to 140% of wild-type levels (Table 1) therefore indicates that the absolute PC contents per leaf area are unaltered and the increased PC:P_{700} ratio is solely attributable to reduced PSI contents per leaf area in the mutant.

The reduced quantum yield of PSII and the reduced amounts of PSI in young expanding leaves of Δ*rpl33* knockout plants provide an explanation for the chilling-sensitive phenotype. Cold stress induces irreversible photoinhibitory damage to PSI due to oxidative destruction of iron-sulfur clusters at the PSI acceptor side (Kudoh and Sonoike, 2002; Scheller and Haldrup, 2005). Thus, the reduced amounts of PSI caused by the reduction in

Table 1. Functional Organization of the Photosynthetic Apparatus in Wild-Type Tobacco and in Δ*rpl33* Plants

Parameter	Wild Type (Mature Leaf)[a]	Δ*rpl33* (Mature Leaf)[a]	Wild Type (Young Expanding Leaf)[b]	Δ*rpl33* (Young Expanding Leaf)[b]
Chlorophyll content (mg m^{-2})	266.1 ± 14.1	250.5 ± 13.9	223.5 ± 7.9	171.5 ± 12.4
Chlorophyll a/b	3.80 ± 0.04	3.41 ± 0.03	3.79 ± 0.11	3.35 ± 0.09
F_v/F_m[c]	0.81 ± 0.00	0.78 ± 0.01	0.79 ± 0.01	0.65 ± 0.04
Assimilation (μmol CO_2 m^{-2} s^{-1})	23.9 ± 1.4	20.6 ± 1.0	–	–
PSII [mmoles (mol chlorophyll)$^{-1}$]	2.22 ± 0.17	2.08 ± 0.08	–	–
Cytochrome bf complex [mmoles (mol chlorophyll)$^{-1}$]	1.09 ± 0.04	1.02 ± 0.04	–	–
PC/PSI[d]	3.09 ± 0.14	3.65 ± 0.28	3.55 ± 0.35	4.90 ± 0.90
PSI [mmoles (mol chlorophyll)$^{-1}$]	2.26 ± 0.03	2.22 ± 0.02	–	–
P_{700} (leaf) [ΔI/I × 10^{-3} (mg chlorophyll)$^{-1}$][e]	47.3 ± 0.1	43.0 ± 1.6	39.0 ± 1.9	33.8 ± 5.1

[a] Measurements were performed on mature leaves (length > 10 cm).
[b] Measurements were performed on young expanding leaves (length < 5 cm). Due to the small leaf sizes of expanding leaves, no thylakoids could be isolated, so that exact quantifications of the photosynthetic complexes were only performed on mature leaves.
[c] F_v, variable fluorescence; F_m, maximum fluorescence.
[d] The PC contents relative to P_{700} were measured in vivo on intact leaves.
[e] The transmission changes (ΔI/I) of P_{700} measured on intact leaves can be used as an indirect measure of PSI content per chlorophyll, assuming that leaf architecture and, thus, length of the optical path within the leaves is comparable for wild-type and knockout plants.

translational capacity in developing leaves of the mutant are most likely responsible for the observed photooxidative damage during recovery from chilling (Figures 8B and 8D). Consistent with this interpretation, photooxidative damage was most severe in those leaves that were youngest during incubation in the cold (e.g., the middle leaf pair in Figure 8B). As PSII is known to require particularly high levels of protein biosynthesis (due to the constant requirement for repair synthesis of the D1 protein; Kanervo et al., 2007), it is conceivable that PSII also contributes to the development of the mutant phenotype after cold stress (Nishiyama et al., 2001; Grennan and Ort, 2007). This interpretation would also be consistent with the reduced F_v/F_m value measured in the knockout mutant (Table 1).

Photosynthesis under Chilling Stress

To explore the physiological basis of the observed chilling sensitivity of the Δ*rpl33* knockout plants in greater detail, we followed key photosynthetic parameters over time in cold stress experiments (Figure 9). In spite of the subtle differences in photosynthetic parameters measurable between young wild-type and Δ*rpl33* leaves (Table 1), these chilling stress measurements had to be performed on young leaves because mature leaves are irreversibly damaged by chilling and die within a few days after transfer back to standard conditions. This explains the slightly lower F_v/F_m values and chlorophyll content of the knockout mutant compared with the wild type at the beginning of the cold treatment (Figure 9). During the cold stress period, leaf development was arrested and no expansion of the young leaves was observed in either the wild type or the knockout. Interestingly, while leaf chlorophyll content declined in both the wild type and the Δ*rpl33* mutant (Figure 9A), photodamage to PSII (as

deduced from the F_v/F_m values; Figure 9B) and loss of redox-active PSI (as deduced from the contents of the PSI reaction center chlorophyll P_{700}; Figure 9C) were more pronounced in the knockout during the stress treatment. After 5 weeks of chilling stress, PSII was virtually destroyed in the mutant and PSI contents had declined to half of the wild-type amounts (Figures 9B and 9C). This is also reflected by the drastic increase of PC contents relative to PSI (Figure 9D), which is due to (1) PC not being a direct target of chilling stress and (2) PC not being encoded in the chloroplast genome, making it the only protein component of the photosynthetic electron transport chain that is not affected by impaired plastid translation (Figure 9D). After transfer of the plants to recovery conditions, PSII and PSI started to recover (in that their contents per chlorophyll increased) within 2 d in both the wild type and the knockout mutant, as seen from the increase in F_v/F_m and the elevated amounts of redox-active PSI per chlorophyll. In the wild type, this recovery is due to both degradation of damaged complexes and initiation of de novo biogenesis of PSI and PSII. Fast initiation of de novo biogenesis of photosystems is evidenced by an increase in chlorophyll content commencing immediately after the end of the stress treatment (Figure 9A). By contrast, in the Δ*rpl33* mutant, the increase in PSII efficiency and photoactive PSI per chlorophyll is mainly attributable to the degradation of damaged complexes, as evidenced by the further decrease in leaf chlorophyll contents observed after the end of the cold stress period (Figure 9A). This is consistent with published data demonstrating that the majority of damaged PSI is not degraded during the actual cold stress phase. Instead, both degradation of damaged PSI and de novo biogenesis of PSI predominantly occur during the early phase of recovery (Zhang and Scheller, 2004). Therefore, the drop in the chlorophyll content in the Δ*rpl33* mutant after transfer back to
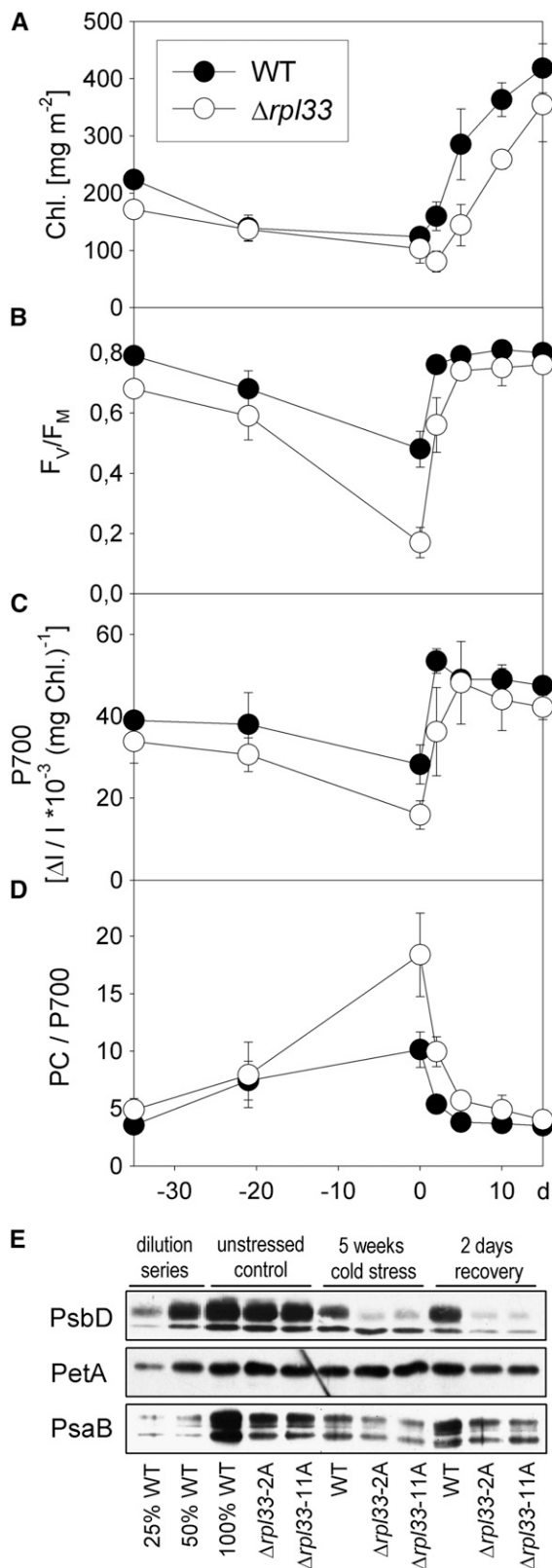
Figure 9. Physiological Analysis of Wild-Type and Δ*rpl33* Plants during Chilling Stress and the Subsequent Recovery Phase.

standard growth conditions (Figure 9A) indicates that (1) more degradation of damaged PSI and PSII occurs than in the wild type and (2) the capacity for de novo biogenesis in the mutant is insufficient to compensate for the degradation of defective photosystems. Enhanced cold-induced photooxidative damage to both photosystems in the Δ*rpl33* mutant was additionally confirmed by immunoblot analysis (Figure 9E). While PetA, the cytochrome f subunit of the cytochrome b$_6$f complex, was unaffected by cold stress in both the wild type and the mutants, the amounts of the PSII subunit PsbD and the PSI subunit PsaB declined under cold stress, and this decline was significantly more pronounced in Δ*rpl33* mutant plants than in wild-type plants (Figure 9E). Taken together, these data indicate that, in the absence of the L33 protein, chloroplast protein biosynthesis capacity is insufficient to counterbalance photooxidative damage to the photosystems in the cold. This explains the delayed recovery of the photosynthetic apparatus from chilling stress, the chilling-sensitive bleached phenotype of the Δ*rpl33* plants, and the postponed reinitiation of growth in the mutant (Figures 8 and 9).

Photosynthesis under Light Stress

Finally, we wanted to test whether or not other stress conditions that cause a high demand for plastid protein biosynthesis would result in similar effects on PSI and PSII activities in the Δ*rpl33* mutant plants. To this end, we shifted wild-type and mutant plants to high-light conditions (1000 μmol m^{-2} s^{-1}) and followed PSII and PSI activities by spectroscopic measurements (Figure 10). This analysis revealed no significant difference between the wild-type and Δ*rpl33* mutant plants (Figure 10) and was therefore consistent with our phenotypic assay under high-light conditions. Likewise, no difference was observed between the wild

Young plants were exposed to cold stress at 4°C for 35 d and then transferred back to standard conditions. Recovery from the stress was followed for 15 d. The end of cold stress was set to day 0. Data represent the means of three wild-type plants and six mutant plants, respectively. The error bars indicate SD. Open circles, Δ*rpl33* plants; closed circles, wild-type plants.
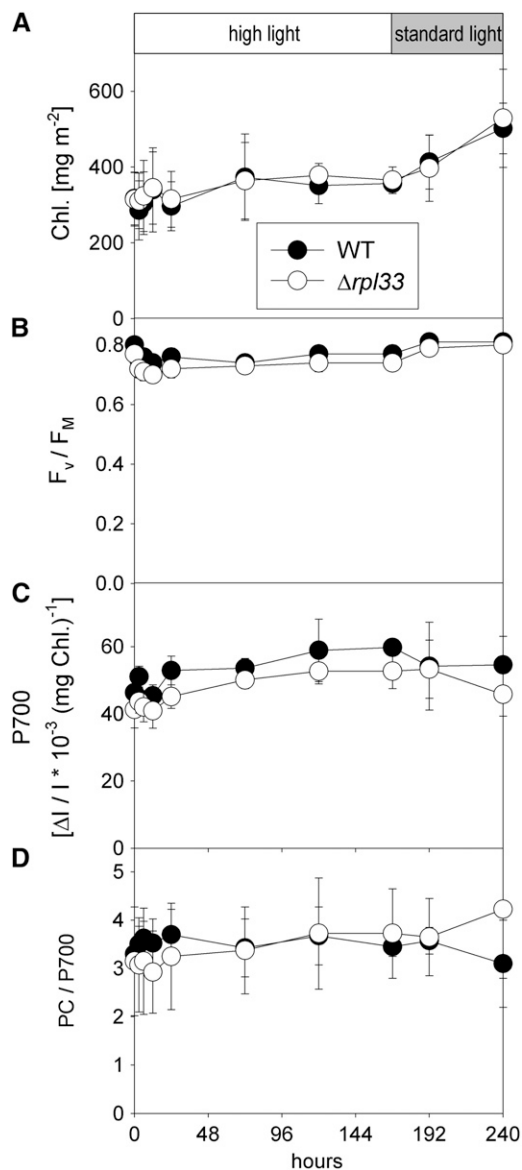
(A) Chlorophyll content.

(B) Quantum yield of dark-adapted PSII (F$_v$/F$_m$).

(C) PSI content determined as the content of the reaction center chlorophyll P$_{700}$ (normalized to leaf chlorophyll contents).

(D) Ratio of the concentration of the soluble electron carrier PC to the concentration of P$_{700}$. While PC content remains relatively stable, P$_{700}$ content decreases in the mutant at the end of the stress phase, resulting in an increase in the PC:P$_{700}$ ratio.

(E) Assessment of cold stress–induced photooxidative damage to the photosystems by immunoblotting. Specific antibodies against diagnostic subunits of PSII (PsbD), the cytochrome b$_6$f complex (PetA), and PSI (PsaB) were used to determine complex accumulation in the wild type and two independently generated Δ*rpl33* lines prior to the stress treatment (unstressed control), after 5 weeks of cold stress at 4°C and after a 2-d recovery period. Protein loading was normalized to leaf chlorophyll contents. Note that, while the spectroscopic measurements (**[B]** to **[D]**) determine photosynthetic complex activities, the immunoblot analyses determine complex accumulation, two parameters that do not always strictly correlate.

Figure 10. Physiological Analysis of Wild-Type and Δ*rpl33* Plants during High-Light Treatment and the Subsequent Recovery Phase.

Young plants were exposed to high-light treatment at 1000 μmol m^{-2} s^{-1} for 7 d (168 h) and then transferred back to standard conditions (standard light; 250 μmol m^{-2} s^{-1}). Data represent the means of three wild-type plants and six mutant plants. Error bars indicate SD. Open circles, Δ*rpl33* plants; closed circles, wild-type plants.
(A) Chlorophyll content.
(B) Quantum yield of dark-adapted PSII (F_v/F_m).
(C) PSI content determined as the content of the reaction center chlorophyll P_{700} (normalized to leaf chlorophyll contents).
(D) Ratio of the concentrations of the soluble electron carrier PC and P_{700}.

type and the Δ*rpl33* mutant when plants were exposed to acute high-light stress (for 1 h at 2000 μmol m^{-2} s^{-1}) followed by analysis of the relaxation kinetics of nonphotochemical quenching (Krause and Weis, 1991). The contribution of qI, a measure of PSII photoinhibition, to the nonphotochemical quenching was

not significantly different under acute high-light stress between the wild type (qI = 0.43) and the Δ*rpl33* mutant (qI = 0.45).

DISCUSSION

In this work, we have taken a reverse genetics approach to assess the functions of plastid-encoded ribosomal proteins that are not strictly conserved across all lineages of evolution. Lack of phylogenetic conservation can have two possible causes: (1) the gene has been lost because it is functionally dispensable, or (2) the gene has been transferred from the plastid genome to the nuclear genome. Although the absence of the plastid genes for the ribosomal proteins tested here (*rps2*, *rps4*, *rpl20*, and *rpl33*) from some lineages of evolution often correlated with loss of photosynthesis and transition to either heterotrophic or parasitic lifestyles, our data reveal that there is probably no direct causal relationship between the loss of photosynthesis, the concomitantly reduced demand for plastid translational capacity and the loss of these ribosomal protein genes from the plastid genome. Instead, the indispensable nature of *rps2* and *rpl20* may suggest that these genes have been transferred to the nuclear genome in those lineages where they are not present in the plastid genome (Timmis et al., 2004; Bock, 2006; Bock and Timmis, 2008).

In addition to components of the translational machinery (Rogalski et al., 2006, 2008; Legen et al., 2007), several other genes of the plastid genome are known to be essential for cell viability in tobacco. These include *ycf1* and *ycf2* (two large hypothetical chloroplast open reading frames of unknown function; Drescher et al., 2000), *clpP* (encoding the proteolytic P subunit of the caseinolytic ATP-dependent protease Clp; Shikanai et al., 2001), and *accD* (encoding the D subunit of the plastid acetyl-CoA carboxylase; Kode et al., 2005). By contrast, all genes encoding components of the photosynthetic apparatus are dispensable, at least under heterotrophic growth conditions (Ruf et al., 1997; Hager et al., 1999). Similarly, all the subunits of the plastid-encoded RNA polymerase are dispensable (Allison et al., 1996). This is because a second transcriptional activity in plastids comes from at least one nuclear-encoded bacteriophage-type RNA polymerase (Liere and Börner, 2007).

Among the four ribosomal protein genes targeted by reverse genetics in this study, only *rpl33* was found to be nonessential. Comparative mass spectrometric identification of ribosomal proteins revealed that this finding cannot be explained by transfer of a functional gene copy to the nuclear genome. Surprisingly, *rpl33* knockout plants displayed no discernable phenotype under standard growth conditions and a variety of different light regimes tested (Figures 6 and 10). Although subtle shifts in the polysome profiles were seen (Figure 7) and a reduction in photosynthetic protein complex accumulation in young developing leaves was measured (Table 1), this did not translate into a noticeable effect on growth of either Δ*rpl33* mutant seedlings or mature plants (Figure 6). The only experimental condition that elicited a strong phenotypic effect was chilling stress at 4°C, suggesting that the lack of the chloroplast L33 protein renders plants sensitive to chilling. It is noteworthy in this respect that *rpl33* loss-of-function mutants found in *E. coli* (Sims and Wild, 1976; Butler and Wild, 1984; Maguire and Wild, 1997) also

displayed a cold-sensitive phenotype (Dabbs, 1991), suggesting that the cold stress–related function of L33 in translation has been evolutionarily conserved. However, *E. coli rpl33* null mutants showed no measurable effect on translation in cells growing exponentially under normal conditions (Sims and Wild, 1976; Butler and Wild, 1984; Maguire and Wild, 1997), which is different from the situation in plants, where young expanding leaves show slightly reduced protein synthesis rates, as evidenced by a slightly delayed biogenesis of the photosynthetic complexes (Table 1). While this effect is phenotypically irrelevant under standard growth conditions, it becomes significant under cold stress conditions (Figure 8). Together with the subtle changes detectable in the polysome profiles (Figure 7), this suggests that the lack of the L33 protein may manifest itself under conditions where the maximum translational capacity of the plastid is needed, such as during reinitiation of protein biosynthesis after cold-induced photooxidative damage.

Our finding that a chloroplast genome-encoded gene is involved in plant tolerance to low-temperature stress is surprising. All previously reported chilling-sensitive mutants exhibited Mendelian inheritance of the mutated locus (e.g., Provart et al., 2003), demonstrating that the affected gene resides in the nuclear genome. Interestingly, one of the previously isolated nuclear chilling-sensitive mutants in *Arabidopsis* (*chs1*) displayed reduced chloroplast protein accumulation in the cold (Schneider et al., 1995), lending circumstantial support to a link between chloroplast translation and chilling tolerance. It is also noteworthy in this respect that several nuclear mutants in maize (*Zea mays*), such as *hcf7* (for *high chlorophyll fluorescence mutant7*) and the virescent mutant *v16* exhibited defects in chloroplast translation that became much more severe when the growth temperature was shifted from 25° to 20°C or 17°C (Hopkins and Elfman, 1984; Barkan, 1993).

The involvement of a chloroplast gene in plant survival under cold stress conditions illustrates a limitation of the forward genetics approaches that are usually taken to isolate stress-hypersensitive mutants. Although some chemicals (such as *N*-nitroso-*N*-methylurea) are known to induce mutations in plastid genomes, neither the generally used chemical mutagen ethyl methanesulfonate nor T-DNA insertional mutagenesis are suitable to induce mutations in organellar genes, leaving the potential contributions of plastid and mitochondrial gene products to stress biology unrecognized.

The high-resolution structure of the large ribosomal subunit of the eubacterial ribosome revealed that the L33 protein forms part of the E site (exit site) of the ribosome (Harms et al., 2001). The E site accommodates the deacylated tRNA and represents the position where the tRNA resides before it leaves the ribosome. It seems conceivable that lack of the L33 protein causes a slightly reduced efficiency of discharged tRNA release from the ribosome. Such a delay in ejection of deacylated tRNAs would also explain the slightly lower mRNA coverage with ribosomes observed in our *rpl33* knockout plants (Figure 7) because it would be expected to have a direct impact on the rate of translation elongation.

Interestingly, the *rpl33* gene has degraded into a pseudogene in the plastid genome of the common bean *P. vulgaris* (Guo et al., 2007). It is noteworthy in this respect that, compared with other legume species, *Phaseolus* is exceptionally chilling sensitive (Wolfe, 1991). It is thus tempting to speculate that the evolutionary degradation of the nonessential chloroplast *rpl33* gene is causally responsible for the high chilling sensitivity of *P. vulgaris*. Although, due to technical reasons, transformation of the chloroplast genome is not yet feasible in *P. vulgaris*, restoration of an intact *rpl33* gene may be a valid future strategy to engineer chilling tolerance in this important food crop.

In summary, our data suggest that plastid protein biosynthesis capacity represents a crucial factor in plant cold stress tolerance and implicate the chloroplast and plastid genome-encoded genes in plant fitness and survival at low temperatures.

METHODS

Plant Material, Growth Conditions, and Phenotype Assays

Tobacco plants (*Nicotiana tabacum* cv Petit Havana) were grown under aseptic conditions on agar-solidified Murashige and Skoog medium containing 30 g/L sucrose (Murashige and Skoog, 1962). Transplastomic lines were rooted and propagated on the same medium. For seed production and analysis of plant phenotypes, *rps2*, *rps4*, *rpl20*, and *rpl33* knockout plants were grown in soil under standard greenhouse conditions. Inheritance and seedling phenotypes were analyzed by germination of surface-sterilized seeds on Murashige and Skoog medium containing 500 mg/L spectinomycin.

Growth tests under different light conditions were performed by raising wild-type and mutant plants from seeds in soil at 26°C under the following light intensities: 50, 200, 600, and 1100 μmol m^{-2} s^{-1}. Heat stress tolerance was assayed by germinating seeds in soil at 26°C followed by transfer to 37°C at 55 μmol m^{-2} s^{-1}. To assess chilling tolerance, seeds were germinated in soil at 26°C and transferred to 4°C after 15 d of growth, where they were cultivated for 5 weeks at 50 μmol m^{-2} s^{-1}.

Construction of Plastid Transformation Vectors

The region of the tobacco plastid genome containing the *rps2* gene (Shinozaki et al., 1986; Figure 2) was isolated as a 3.0-kb *Xho*I/*Spe*I fragment and cloned into the similarly digested vector pUC18. To produce the transformation vector pΔ*rps2*, most of the *rps2* coding region was deleted using the restriction enzymes *Eco*RI and *Kas*I followed by a fill-in reaction with the Klenow fragment of DNA polymerase I from *Escherichia coli*. Finally, the *aadA* cassette (Svab and Maliga, 1993) was inserted into the *rps2* deletion site as an *Ecl*136II/*Dra*I fragment.

The *rps4* gene was isolated from the plastid genome in a 2.7-kb *Eco*RI/ *Xho*I fragment. This fragment was cloned into the pBS KS+ vector using the same restriction enzymes. Subsequently, the *rps4* gene was partially deleted using the restriction enzymes *Hpa*I and *Ppu*MI (Figure 1). The overhanging ends produced by *Ppu*MI were blunted using the Klenow fragment of DNA polymerase I. The final transformation plasmid pΔ*rps4* was obtained by insertion of the *aadA* cassette into the *rps4* deletion site.

The plastome region containing the *rpl20* and *rpl33* genes was cloned as a 3.7-kb *Nde*I/*Eco*RI restriction fragment into the similarly cut pUC18 vector. To generate transformation vector pΔ*rp20*, the plasmid clone was linearized with the restriction enzyme *Nru*I followed by insertion of the *aadA* cassette into the middle of the *rpl20* coding region. Transformation vector pΔ*rpl33* was produced by deletion of the *rpl33* gene via digestion with the restriction enzymes *Msc*I and *Bsm*FI. The overhanging ends generated by *Bsm*FI were subsequently blunted using the Klenow fragment of DNA polymerase I and the *aadA* cassette was ligated into the *rpl33* deletion site.

Plastid Transformation and Selection of Transplastomic Tobacco Lines

Young leaves from sterile tobacco plants were bombarded with plasmid-coated 0.6 μm gold particles using a helium-driven biolistic gun (PDS1000He; Bio-Rad). Primary spectinomycin-resistant lines were selected from 5 × 5-mm leaf pieces on plant regeneration medium containing 500 mg/L spectinomycin (Svab and Maliga, 1993). Spontaneous spectinomycin-resistant plants were eliminated by double selection tests on medium containing spectinomycin and streptomycin (500 mg/L each; Svab and Maliga, 1993; Bock, 2001). Several independent transplastomic lines were subjected to four additional rounds of regeneration on spectinomycin-containing regeneration medium to enrich for the transplastome and to select for homoplasmy.

Isolation of Nucleic Acids and Hybridization Procedures

Total plant DNA was isolated by a cetyltrimethylammoniumbromide-based method (Doyle and Doyle, 1990). DNA samples were digested with restriction enzymes, separated on 0.8% agarose gels, and blotted onto Hybond N nylon membranes (GE Healthcare). For hybridization, [α-^{32}P] dATP-labeled probes were generated by random priming (Multiprime DNA labeling kit; GE Healthcare). Restriction fragments covering part of the *rps2/rpoC2* genes, *trnT*-UGU/*orf70A*, *rpl20/5′rps12*, and *psaJ/rpl33* region (Figures 1 to 4) were used as probes for the RFLP analyses in *Δrps2*, *Δrps4*, *Δrpl20*, and *Δrpl33* plants, respectively. Hybridizations were performed at 65°C in rapid hybridization buffer (GE Healthcare) following the manufacturer's protocol.

PCR

Presence of recombination products in transplastomic lines was confirmed by PCR amplification using the primers PaadA25 (5′-AGATCAC-CAAGGTAGTCGGCAA-3′) and PtrnH (5′-CTTGATCCACTTGGCTACA-TCC-3′). To confirm the deletion of the *rpl33* gene, combinations of the following primers were used (Figure 4): P5′rpl33 (5′-TCAAAAATCC-AAAGGAGGTTC-3′), PaadA136 (5′-TCGATGACGCCAACTACC-3′), PaadA25 (5′-AGATCACCAAGGTAGTCGGCAA-3′), and P3′rpl33 (5′-CAT-TTTTTCCCCTTCCTTGA-3′). Fifty nanograms of total genomic DNA was amplified in 50-μL reactions in a reaction mixture containing 200 μM of each deoxynucleotide triphosphate, 2.0 mM MgCl$_2$, 10 pmol of each primer, and 1 unit of *Taq* DNA polymerase (Promega). The standard PCR program was 40 cycles of 40 s at 94°C, 90 s at 55°C, and 90 s at 72°C with a 3-min extension of the first cycle at 94°C and a 5-min final extension at 72°C. PCR products were analyzed by gel electrophoresis in 1.5% agarose gels.

Polysome Analysis

Polysomes were purified as described previously (Rogalski et al., 2008). RNA pellets were redissolved in 30 μL water, and aliquots of 1.5 μL were denatured for 5 min at 95°C and then loaded onto denaturing formaldehyde-containing agarose gels for RNA gel blot analysis. mRNA-specific probes for RNA gel blot analysis were prepared from restriction fragments (*rbcL*, 565-bp SacII/PstI fragment) or PCR products: *psbA*, 1020-bp PCR product obtained with primers PpsbA5′(5′-ATAGACTAGGCCAGGATCT-TAT-3′) and PpsbA3′ (5′-ATTTTACCATGACTGCAATTTTAGAG-3′); *psbE* operon, 481-bp PCR product obtained with primers PY (5′-CCTTC-CCTATTCATTGCGGGTTGG-3′) and P7652 (5′-CCGAATGAGCTAAGA-GAATCTT-3′); *psaB*, 550-bp PCR product generated by amplification with primers P7247 (5′-CCCAGAAAGAGGCTGGCCC-3′) and P7244 (5′-CCCAAGGGGCGGGAACTGC-3′).

Ribosome Isolation and Mass Spectrometry

Chloroplasts were isolated as described previously (Rogalski et al., 2008). Chloroplast pellets were resuspended in lysis buffer (3% Triton X-100, 10 mM Tris-HCl, pH 7.6, 50 mM KCl; 10 mM Mg acetate, and 7 mM β-mercaptoethanol). The chloroplast lysate was cleared by centrifugation at 26,000*g* for 30 min. The supernatant was layered onto a 1 M sucrose cushion containing 10 mM Tris-HCl, pH 7.6, 50 mM KCl, 10 mM magnesium acetate, and 7 mM β-mercaptoethanol, and the ribosomes were pelleted by centrifugation at 86,000*g* for 17 h. The pellet was then resuspended in T$_{25}$K$_{100}$M$_5$D$_5$T buffer (25 mM Tris-HCl, pH 8.0, 100 mM NH$_4$Cl, 25 mM MgCl$_2$, and 5 mM DTT; Yamaguchi et al., 2002), layered over 32 mL of a linear sucrose gradient (10 to 30% in T$_{25}$K$_{100}$M$_5$D$_5$T buffer) and centrifuged at 90,000*g* for 5 h. The gradients were then fractionated and the ribosomes were pelleted from the fractions by centrifugation at 110,000*g* for 16 h. Finally, the ribosomes were resuspended in T$_{25}$K$_{100}$M$_5$D$_5$T buffer and frozen at −80°C until further use.

For mass spectrometric protein identification, 40 μg of wild-type and *Δrpl33* chloroplast ribosomes were denatured for 5 min at 95°C and loaded on 16.5% (w/v) SDS-polyacrylamide gels. The gels were stained with colloidal Coomassie Brilliant Blue (Imperial protein stain; Rockford) overnight and destained for 6 to 8 h in distilled water. The region between 5 and 22 kD was cut out from the gel and subsequently divided in 14 gel pieces of ~0.5 cm each. The gel pieces were digested with trypsin following standard procedures (Olsen et al., 2004). Prior to mass spectrometric analysis, tryptic peptides were desalted over stage tips (Ishihama et al., 2006). Tryptic peptide mixtures were analyzed by liquid chromatography–tandem mass spectrometry (MS/MS) using nanoflow HPLC (Proxeon Biosystems) and an Orbitrap hybrid mass spectrometer (LTQ-Orbitrap; Thermo Electron) as mass analyzer. Peptides were eluted from a 75-μm analytical column (Reprosil C18; Dr. Maisch) on a linear gradient running from 4 to 64% acetonitrile in 40 min and sprayed directly into the LTQ-Orbitrap mass spectrometer. Proteins were identified by tandem mass spectrometry (MS/MS) by information-dependent acquisition of fragmentation spectra of multiple-charged peptides. Fragment MS/MS spectra from raw files were extracted as DTA files and then merged to peak lists using default settings of DTASuperCharge version 1.18 (http://msquant.sourceforge.net) with a tolerance for precursor ion detection of 50 ppm. Fragmentation spectra were searched against a nonredundant database consisting of the complete *Arabidopsis thaliana* protein database (TAIR7, version 2007-04; 31,921 entries; www.Arabidopsis.org) to which 21 tobacco ribosomal protein sequences (tobacco chloroplast encoded genes) and major contaminants were added. Alternatively, peak lists were matched against the tobacco transcript assemblies database (http://www.tigr.org/plantgenomics/htdocs/databases.html; Childs et al., 2007) using the Mascot algorithm (version 2.2.0; Matrix Science). The following search parameters were applied: trypsin as cleaving enzyme, peptide mass tolerance 10 ppm, MS/MS tolerance 0.8 D, and one missed cleavage allowed. Carbamido-methylation of Cys was set as a fixed modification, and Met oxidation was chosen as a variable modification. Only peptides with a length of more than five amino acids were considered. In general, peptides were accepted without manual interpretation if they displayed a Mascot score > 32 (as defined by Mascot P < 0.01 significance threshold), and peptides with a score > 20 were manually inspected, requiring a series of three y or b ions to be accepted. Protein abundance was estimated using the exponentially modified protein abundance index (Ishihama et al., 2005).

Gas Exchange Measurements

Leaf assimilation capacities were determined using a Clark-type leaf oxygen electrode (Hansatech Instruments). Measurements were performed on leaf discs (10 cm^2 leaf area) under CO$_2$-saturated conditions (5% CO$_2$). Respiration was measured for 10 min in the dark-adapted leaf.

Then, leaves were illuminated with saturating light (1000 μE m^{-2} s^{-1}) provided by a tungsten lamp (Schott). Photosynthetic oxygen evolution was measured until steady state was attained. Assimilation was corrected for respiration rates, assuming that respiration is unaltered in the light (Fernie et al., 2004).

Chlorophyll Fluorescence Measurements

Chlorophyll fluorescence was recorded with a pulse-amplitude modulated fluorimeter (Dual-PAM; Heinz Walz). Plants were dark adapted for 1 h prior to determination of PSII quantum efficiency (F$_v$/F$_m$). The effect of short-term acute high-light stress was assessed by exposing leaves to a light intensity of 2000 μmol m^{-2} s^{-1} in the Dual-PAM for 1 h, followed by determination of the three components of nonphotochemical quenching (qE, qT, and qI, with qI being a measure of PSII photoinhibition) during a subsequent 15-min relaxation period in the dark (Krause and Weis, 1991).

Difference Absorption Spectroscopy

The contents of PSII, the cytochrome b$_6$f complex, and PSI were determined in thylakoids isolated according to Schöttler et al. (2004). PSI was quantified from P$_{700}$ difference absorption signals at 830- to 870-nm wavelength in solubilized thylakoids (Schöttler et al., 2007b) using the Dual-PAM instrument. PSII and the cytochrome b$_6$f complex were determined from difference absorption measurements of cytochrome b$_{559}$ (PSII) and cytochromes f and b$_6$. Thylakoids equivalent to 50 μg chlorophyll mL^{-1} were incubated in a low-salt medium to improve the optical properties of the sample by unstacking the thylakoids. All cytochromes were oxidized by application of 1 mM sodium ferricyanide. Addition of 10 mM sodium ascorbate resulted in the reduction of cytochrome f and the high-potential form of cytochrome b$_{559}$, while cytochrome b$_6$ and the low-potential form of cytochrome b$_{559}$ were only reduced upon addition of dithionite. At each redox potential, absorption spectra between 575- and 540-nm wavelengths were determined using the V-550 spectrophotometer (Jasco) with a head-on photomultiplier. The monochromator slit width was set to 1 nm. The difference absorption spectra were deconvoluted using reference spectra and difference absorption coefficients as described (Kirchhoff et al., 2002). The PSII content was calculated from the sum of the difference absorption signals arising from the low and high potential forms of cytochrome b$_{559}$.

The relative stoichiometries of PC per P$_{700}$ were determined using the plastocyanin version of the Dual-PAM spectroscope (Dual-PAM-S; Heinz Walz; Schöttler et al., 2007b). Measurements were performed on intact leaves prior to thylakoid isolation because PC is partly released from the thylakoid lumen during the isolation procedure; therefore, data obtained from isolated thylakoids are not fully quantitative.

Protein Gel Electrophoresis and Immunoblotting

Immunodetection of representative subunits of complexes was performed after separation of thylakoid proteins by SDS-polyacrylamide gel electrophoresis as described previously (Schöttler et al., 2007a, 2007b). The separated proteins were transferred onto polyvinylidene difluoride membranes (Hybond P; GE Healthcare) using the tank blot system Perfect Blue Web M (PeqLab) and a standard transfer buffer. Immunobiochemical detection was performed with the ECL Plus protein gel blotting detection system (GE Healthcare) according to the manufacturer's instructions. Antisera against thylakoid proteins were purchased from Agrisera.

Accession Numbers

Sequence data for tobacco plastid ribosomal proteins can be found in the GenBank/EMBL database under the accession number for the tobacco (*N. tabacum*) plastid genome: Z00044.

Supplemental Data

The following materials are available in the online version of this article.

Supplemental Figure 1. Confirmation of Recombination Events in Transplastomic Lines by PCR Analysis.

Supplemental Table 1. Mass Spectrometric Identification of Plastid Ribosomal Proteins in Wild-Type and Δ*rpl33* Plants.

REFERENCES

Ahlert, D., Ruf, S., and Bock, R. (2003). Plastid protein synthesis is required for plant development in tobacco. Proc. Natl. Acad. Sci. USA **100:** 15730–15735.

Albrecht, V., Ingenfeld, A., and Apel, K. (2006). Characterization of the snowy cotyledon 1 mutant of *Arabidopsis thaliana*: The impact of chloroplast elongation factor G on chloroplast development and plant vitality. Plant Mol. Biol. **60:** 507–518.

Allison, L.A., Simon, L.D., and Maliga, P. (1996). Deletion of rpoB reveals a second distinct transcription system in plastids of higher plants. EMBO J. **15:** 2802–2809.

Barkan, A. (1988). Proteins encoded by a complex chloroplast transcription unit are each translated from both monocistronic and polycistronic mRNAs. EMBO J. **7:** 2637–2644.

Barkan, A. (1993). Nuclear mutants of maize with defects in chloroplast polysome assembly have altered chloroplast RNA metabolism. Plant Cell **5:** 389–402.

Barkan, A. (1998). Approaches to investigating nuclear genes that function in chloroplast biogenesis in land plants. Methods Enzymol. **297:** 38–57.

Bock, R. (2001). Transgenic chloroplasts in basic research and plant biotechnology. J. Mol. Biol. **312:** 425–438.

Bock, R. (2006). Extranuclear inheritance: Gene transfer out of plastids. Prog. Bot. **67:** 75–98.

Bock, R. (2007). Structure, function, and inheritance of plastid genomes. Top. Curr. Genet. **19:** 29–63.

Bock, R., and Khan, M.S. (2004). Taming plastids for a green future. Trends Biotechnol. **22:** 311–318.

Bock, R., and Timmis, J.N. (2008). Reconstructing evolution: Gene transfer from plastids to the nucleus. Bioessays **30:** 556–566.

Bungard, R.A. (2004). Photosynthetic evolution in parasitic plants: Insight from the chloroplast genome. Bioessays **26:** 235–247.

Butler, P.D., and Wild, D.G. (1984). Ribosomal protein synthesis by a mutant of *Escherichia coli*. Eur. J. Biochem. **144:** 649–654.

Childs, K.L., Hamilton, J.P., Zhu, W., Ly, E., Cheung, F., Wu, H., Rabinowicz, P.D., Town, C.D., Buell, C.R., and Chan, A.P. (2007).

The TIGR plant transcript assemblies database. Nucleic Acids Res. **35:** D846–D851.

Dabbs, E.R. (1991). Mutants lacking individual ribosomal proteins as a tool to investigate ribosomal properties. Biochimie **73:** 639–645.

de Koning, A.P., and Keeling, P.J. (2006). The complete plastid genome sequence of the parasitic green alga Helicosporidium sp. is highly reduced and structured. BMC Biol. **4:** 1–10.

Doyle, J.J., and Doyle, J.L. (1990). Isolation of plant DNA from fresh tissue. Focus **12:** 13–15.

Drescher, A., Ruf, S., Calsa, T., Jr., Carrer, H., and Bock, R. (2000). The two largest chloroplast genome-encoded open reading frames of higher plants are essential genes. Plant J. **22:** 97–104.

Falk, J., Schmidt, A., and Krupinska, K. (1993). Characterization of plastid DNA transcription in ribosome deficient plastids of heat-bleached barley leaves. J. Plant Physiol. **141:** 176–181.

Feierabend, J. (1992). Conservation and structural divergence of organellar DNA and gene expression in non-photosynthetic plastids during ontogenetic differentiation and phylogenetic adaption. Bot. Acta **105:** 227–231.

Fernie, A.R., Carrari, F., and Sweetlove, L.J. (2004). Respiratory metabolism: Glycolysis, the TCA cycle and mitochondrial electron transport. Curr. Opin. Plant Biol. **7:** 254–261.

Gockel, G., Hachtel, W., Baier, S., Fliss, C., and Henke, M. (1994). Genes for components of the chloroplast translational apparatus are conserved in the reduced 73-kb plastid DNA of the nonphotosynthetic euglenoid flagellate *Astasia longa*. Curr. Genet. **26:** 256–262.

Grennan, A.K., and Ort, D.R. (2007). Cool temperatures interfere with D1 synthesis in tomato by causing ribosomal pausing. Photosynth. Res. **94:** 375–385.

Guo, X., Castillo-Ramírez, S., González, V., Bustos, P., Fernández-Vázquez, J.L., Santamaría, R.I., Arellano, J., Cevallos, M.A., and Dávila, G. (2007). Rapid evolutionary change of common bean (*Phaseolus vulgaris* L) plastome, and the genomic diversification of legume chloroplasts. BMC Genomics **8:** 228.

Hager, M., Biehler, K., Illerhaus, J., Ruf, S., and Bock, R. (1999). Targeted inactivation of the smallest plastid genome-encoded open reading frame reveals a novel and essential subunit of the cytochrome b6f complex. EMBO J. **18:** 5834–5842.

Hallick, R.B., Hong, L., Drager, R.G., Favreau, M.R., Monfort, A., Orsat, B., Spielmann, A., and Stutz, E. (1993). Complete sequence of *Euglena gracilis* chloroplast DNA. Nucleic Acids Res. **21:** 3537–3544.

Harms, J., Schluenzen, F., Zarivach, R., Bashan, A., Gat, S., Agmon, I., Bartels, H., Franceschi, F., and Yonath, A. (2001). High resolution structure of the large ribosomal subunit from a mesophilic eubacterium. Cell **107:** 679–688.

Hopkins, W.G., and Elfman, B. (1984). Temperature-induced chloroplast ribosome deficiency in virescent maize. J. Hered. **75:** 207–211.

Ishihama, Y., Oda, Y., Tabata, T., Sato, T., Nagasu, T., Rappsilber, J., and Mann, M. (2005). Exponentially Modified Protein Abundance Index (emPAI) for estimation of absolute protein amount in proteomics by the number of sequenced peptides per protein. Mol. Cell. Proteomics **4:** 1265–1272.

Ishihama, Y., Rappsilber, J., and Mann, M. (2006). Modular Stop and Go Extraction Tips with stacked disks for parallel and multidimensional peptide fractionation in proteomics. J. Proteome Res. **5:** 988–994.

Kaczanowska, M., and Rydén-Aulin, M. (2007). Ribosome biogenesis and the translation process in *Escherichia coli*. Microbiol. Mol. Biol. Rev. **71:** 477–494.

Kanervo, E., Suorsa, M., and Aro, E.-M. (2007). Assembly of protein complexes in plastids. Top. Curr. Genet. **19:** 283–313.

Kirchhoff, H., Mukherjee, U., and Galla, H.J. (2002). Molecular archi-tecture of the thylakoid membrane: Lipid diffusion space for plasto-quinone. Biochemistry **41:** 4872–4882.

Kode, V., Mudd, E.A., Iamtham, S., and Day, A. (2005). The tobacco plastid accD gene is essential and is required for leaf development. Plant J. **44:** 237–244.

Krause, G.H., and Weis, E. (1991). Chlorophyll fluorescence and photosynthesis: The basics. Annu. Rev. Plant Physiol. Plant Mol. Biol. **42:** 313–349.

Kudoh, H., and Sonoike, K. (2002). Irreversible damage to photosystem I by chilling in the light: cause of the degradation of chlorophyll after returning to normal growth temperature. Planta **215:** 541–548.

Legen, J., Wanner, G., Herrmann, R.G., Small, I., and Schmitz-Linneweber, C. (2007). Plastid tRNA genes trnC-GCA and trnN-GUU are essential for plant cell development. Plant J. **51:** 751–762.

Liere, K., and Börner, T. (2007). Transcription and transcriptional regulation in plastids. Top. Curr. Genet. **19:** 121–174.

Maguire, B.A., and Wild, D.G. (1997). The roles of proteins L28 and L33 in the assembly and function of *Escherichia coli* ribosomes in vivo. Mol. Microbiol. **23:** 237–245.

Maliga, P. (2004). Plastid transformation in higher plants. Annu. Rev. Plant Biol. **55:** 289–313.

Manuell, A.L., Quispe, J., and Mayfield, S.P. (2007). Structure of the chloroplast ribosome: Novel domains for translation regulation. PLoS Biol. **5:** 1785–1797.

Murashige, T., and Skoog, F. (1962). A revised medium for rapid growth and bio assays with tobacco tissue culture. Physiol. Plant. **15:** 473–497.

Nishiyama, Y., Yamamoto, H., Allakhverdiev, S.I., Inaba, M., Yokota, A., and Murata, N. (2001). Oxidative stress inhibits the repair of photodamage to the photosynthetic machinery. EMBO J. **20:** 5587–5594.

Olsen, J.V., Ong, S.E., and Mann, M. (2004). Trypsin cleaves exclusively C-terminal to arginine and lysine residues. Mol. Cell. Proteomics **3:** 608–614.

Peled-Zehavi, H., and Danon, A. (2007). Translation and translational regulation in chloroplasts. Top. Curr. Genet. **19:** 249–281.

Provart, N.J., Gil, P., Chen, W., Han, B., Chang, H.-S., Wang, X., and Zhu, T. (2003). Gene expression phenotypes of Arabidopsis associated with sensitivity to low temperatures. Plant Physiol. **132:** 893–906.

Rogalski, M., Karcher, D., and Bock, R. (2008). Superwobbling facilitates translation with reduced tRNA sets. Nat. Struct. Mol. Biol. **15:** 192–198.

Rogalski, M., Ruf, S., and Bock, R. (2006). Tobacco plastid ribosomal protein S18 is essential for cell survival. Nucleic Acids Res. **34:** 4537–4545.

Ruf, S., Kössel, H., and Bock, R. (1997). Targeted inactivation of a tobacco intron-containing open reading frame reveals a novel chloroplast-encoded photosystem I-related gene. J. Cell Biol. **139:** 95–102.

Scheller, H.V., and Haldrup, A. (2005). Photoinhibition of photosystem I. Planta **221:** 5–8.

Schneider, J.C., Nielsen, E., and Somerville, C. (1995). A chilling-sensitive mutant of Arabidopsis is deficient in chloroplast protein accumulation at low temperature. Plant Cell Environ. **18:** 23–32.

Schöttler, M.A., Flügel, C., Thiele, W., and Bock, R. (2007a). Knock-out of the plastid-encoded PetL subunit results in reduced stability and accelerated leaf age-dependent loss of the cytochrome b$_6$f complex. J. Biol. Chem. **282:** 976–984.

Schöttler, M.A., Flügel, C., Thiele, W., Stegemann, S., and Bock, R. (2007b). The plastome-encoded PsaJ subunit is required for efficient photosystem I excitation, but not for plastocyanin oxidation in tobacco. Biochem. J. **403:** 251–260.

Schöttler, M.A., Kirchhoff, H., and Weis, E. (2004). The role of

plastocyanin in the adjustment of the photosynthetic electron transport to the carbon metabolism in tobacco. Plant Physiol. **136:** 4265–4274.

Sharma, M.R., Wilson, D.N., Datta, P.P., Barat, C., Schluenzen, F., Fucini, P., and Agrawal, R.K. (2007). Cryo-EM study of the spinach chloroplast ribosome reveals the structural and functional roles of plastid-specific ribosomal proteins. Proc. Natl. Acad. Sci. USA **104:** 19315–19320.

Shikanai, T., Shimizu, K., Ueda, K., Nishimura, Y., Kuroiwa, T., and Hashimoto, T. (2001). The chloroplast cplP gene, encoding a proteolytic subunit of ATP-dependent protease, is indispensable for chloroplast development in tobacco. Plant Cell Physiol. **42:** 264–273.

Shinozaki, K., et al. (1986). The complete nucleotide sequence of the tobacco chloroplast genome: Its gene organization and expression. EMBO J. **5:** 2043–2049.

Sims, P.F.G., and Wild, D.G. (1976). Peptidyltransferase activity of ribosomes and a ribosome precursor from a mutant of *Escherichia coli*. Biochem. J. **160:** 721–726.

Svab, Z., and Maliga, P. (1993). High-frequency plastid transformation in tobacco by selection for a chimeric aadA gene. Proc. Natl. Acad. Sci. USA **90:** 913–917.

Timmis, J.N., Ayliffe, M.A., Huang, C.Y., and Martin, W. (2004). Endosymbiotic gene transfer: organelle genomes forge eukaryotic chromosomes. Nat. Rev. Genet. **5:** 123–136.

Wakasugi, T., Tsudzuki, T., and Sugiura, M. (2001). The genomics of land plant chloroplasts: gene content and alteration of genomic information by RNA editing. Photosynth. Res. **70:** 107–118.

Wilson, R.J.M. (2002). Progress with parasite plastids. J. Mol. Biol. **319:** 257–274.

Wilson, R.J.M., and Williamson, D.H. (1997). Extrachromosomal DNA in the Apicomplexa. Microbiol. Mol. Biol. Rev. **61:** 1–16.

Wilson, R.J.M., Denny, P.W., Preiser, P.R., Rangachari, K., Roberts, K., Roy, A., Whyte, A., Strath, M., Moore, D.J., Moore, P.W., and Williamson, D.H. (1996). Complete gene map of the plastid-like DNA of the malaria parasite *Plasmodium falciparum*. J. Mol. Biol. **261:** 155–172.

Wolfe, D.W. (1991). Low temperature effects on early vegetative growth, leaf gas exchange and water potential of chilling-sensitive and chilling-tolerant crop species. Ann. Bot. (Lond.) **67:** 205–212.

Yamaguchi, K., Prieto, S., Beligni, M.V., Haynes, P.A., McDonald, W. H., Yates III, J.R., and Mayfield, S.P. (2002). Proteomic characterization of the small subunit of *Chlamydomonas reinhardtii* chloroplast ribosome: Identification of a novel S1 domain-containing protein and unusually large orthologs of bacterial S2, S3, and S5. Plant Cell **14:** 2957–2974.

Yamaguchi, K., and Subramanian, A.R. (2000). The plastid ribosomal proteins. J. Biol. Chem. **275:** 28466–28482.

Yamaguchi, K., von Knoblauch, K., and Subramanian, A.R. (2000). The plastid ribosomal proteins. J. Biol. Chem. **275:** 28455–28465.

Zhang, S., and Scheller, H.V. (2004). Photoinhibition of photosystem I at chilling temperature and subsequent recovery in *Arabidopsis thaliana*. Plant Cell Physiol. **45:** 1595–1602.

This information is current as of March 28, 2012

References	This article cites 69 articles, 22 of which can be accessed free at: http://www.plantcell.org/content/20/8/2221.full.html#ref-list-1
Permissions	https://www.copyright.com/ccc/openurl.do?sid=pd_hw1532298X&issn=1532298X&WT.mc_id=pd_hw1532298X
eTOCs	Sign up for eTOCs at: http://www.plantcell.org/cgi/alerts/ctmain
CiteTrack Alerts	Sign up for CiteTrack Alerts at: http://www.plantcell.org/cgi/alerts/ctmain
Subscription Information	Subscription Information for *The Plant Cell* and *Plant Physiology* is available at: http://www.aspb.org/publications/subscriptions.cfm